GEOPHYSICAL RESEARCH LETTERS, VOL. ???, XXXX, DOI:10.1029/,

Flux Transfer Event observation at Saturn's dayside magnetopause by the Cassini spacecraft

Jamie M. Jasinski,[1,2,3] James A. Slavin,[1] Christopher S. Arridge,[4]

Gangkai Poh,[1] Xianzhe Jia,[1] Nick Sergis,[5] Andrew J. Coates,[2,3]

Geraint H. Jones,[2,3] and J. Hunter Waite Jr.[6]

Author Manuscript

This is the author manuscript accepted for publication and has undergone full peer review but has not been through the copyediting, typesetting, pagination and proofreading process, which may lead to differences between this version and the Version of Record. Please cite this article as doi: 10.1002/2016GL069260

This article is protected by copyright. All rights reserved.

[1]Dept. of Climate and Space Sciences and Engineering, University of Michigan, Ann Arbor, MI, USA.

[2]Mullard Space Science Laboratory, University College London, UK.

[3]The Centre for Planetary Sciences at UCL/Birkbeck, London, UK.

[4]Dept. of Physics, Lancaster University, Lancaster, UK.

[5]Office for Space Research and Technology, Academy of Athens, Athens, Greece.

[6]Southwest Research Institute, San Antonio, Texas, USA.

Author Manuscript

This article is protected by copyright. All rights reserved.

Abstract

We present the first observation of a flux rope at Saturn's dayside magnetopause. This is an important result because it shows that the Saturnian magnetopause is conducive to multiple x-line reconnection and flux rope generation. Minimum variance analysis shows the magnetic signature is consistent with a flux rope. The magnetic observations were well-fitted to a constant-α force-free flux rope model. The radius and magnetic flux content of the rope is estimated to be 4600-8300 km and 0.2-0.8 MWb, respectively. Cassini also observed five travelling compression regions (remote signatures of flux ropes), in the adjacent magnetosphere. The magnetic flux content is compared to other estimates of flux opening via reconnection at Saturn.

Author Manuscript

This article is protected by copyright. All rights reserved.

1. Introduction

Flux transfer events (FTEs) are twisted flux tubes first observed at Earth's magnetopause by the ISEE 1 and 2 spacecraft [*Russell and Elphic*, 1978, 1979]. FTEs consist of a flux rope (FR), which have been postulated to form as a result of simultaneous magnetic reconnection occurring at multiple x-lines [*Fu and Lee*, 1985] sandwiched between compressed draped interplanetary magnetic field (shown in Figure 1a) and the dayside magnetospheric field [*Zhang et al.*, 2012; *Zhong et al.*, 2013]. Other flux-rope-generation mechanisms include a change in the reconnection rate at a single x-line [*Southwood et al.*, 1988; *Scholer*, 1988], and bursts of reconnection at a spatially narrow site that produce two 'elbow-shaped' FTEs [*Russell and Walker*, 1985].

The twisting of a flux tube leads to a bipolar signature observed in the direction normal to the axis of the flux rope (the basic observational signature) in the magnetic field measurements. This is detected alongside an increase in magnetic field strength in the axial direction at the centre of the flux rope (due to its structure, shown Figure 1b). If the spacecraft does not cross through the FTE, but passes near the edges, then only magnetic flux draped about the FTE is observed (shaded red in Figure 1a). This signature is termed a travelling compression region or TCR [*Zhang et al.*, 2008; *Slavin et al.*, 2012]. The observation of FTEs is common at the terrestrial planets and they have been studied at the magnetopause at Earth [e.g. *Russell and Elphic*, 1978; *Fear et al.*, 2005, 2008; *Owen et al.*, 2008; *Varsani et al.*, 2014], Mercury [e.g. *Russell and Walker*, 1985; *Slavin et al.*, 2009, 2010; *Imber et al.*, 2014] and Jupiter [*Walker and Russell*, 1985; *Huddleston et al.*, 1997]. They have also been observed in the ionospheres of Venus and Mars [*Elphic et al.*,

Author Manuscript

This article is protected by copyright. All rights reserved.

1980; *Vignes et al.*, 2004], and downstream of Mars' large crustal anomalies [*Brain et al.*, 2010].

The role of reconnection in driving the magnetosphere, and the extent to which it opens and closes magnetic flux at Saturn is a controversial topic. Theory indicates that the occurrence and rate of reconnection is determined by the magnetic shear between the two magnetic fields and the plasma β (the thermal to magnetic pressure ratio) [*Quest and Coroniti*, 1981; *Swisdak et al.*, 2003, 2010]. The relatively low plasma β of $\sim$1, typical of the Earth's magnetosheath, results in reconnection occurring at shear angles of $\sim 90° - 270°$ [*Trenchi et al.*, 2008], with the highest reconnection rates observed with anti-parallel fields [*Burton et al.*, 1975; *Mozer and Retinò*, 2007]. Large differences in plasma β across the magnetopause tend to occur during high Alfvénic Mach number (M_A) conditions in the solar wind, which produce high-β magnetosheaths [e.g. *Slavin et al.*, 1984; *Gershman et al.*, 2013]. In comparison, lower M_A in the solar wind at Mercury greatly reduces the β in the magnetosheath. For low-β conditions, reconnection is possible for very low shear angles [*Slavin et al.*, 2009, 2014; *DiBraccio et al.*, 2013].

At Saturn, *Masters et al.* [2012] investigated Cassini magnetopause crossings, and found that for the majority of the observations, the conditions at the magnetopause were not conducive to reconnection. This is supported by the lack of any dayside FTE observations to date after over 11 years of Cassini orbiting Saturn. Evidence for FTEs at Jupiter have been reported [*Russell*, 1995; *Huddleston et al.*, 1997] but not at Saturn where a statistical search for FTEs found none [*Lai et al.*, 2012]. The low-latitude boundary layer between the magnetopause and the magnetosphere at Saturn has been observed not to vary in

This article is protected by copyright. All rights reserved.

thickness for different interplanetary magnetic field (IMF) orientations [*Masters et al.*, 2011a, b], unlike at Earth where it is found to be thinner when the IMF is anti-parallel to the magnetospheric field (due to the erosion of the open magnetic field lines) [e.g. *Šafránková et al.*, 2007]. The magnetopause position at Saturn was not found to depend upon the IMF direction [*Lai et al.*, 2012], unlike at Earth and Jupiter [*Aubry et al.*, 1970; *Kivelson and Southwood*, 2003].

However, this is not to say that reconnection does not occur at all at Saturn, but it is not as common as at Earth, is not triggered under the same conditions, and that its effect on the dynamics of the Saturnian magnetosphere may not necessarily be analogous to the terrestrial system. Modeling of the possible areas where reconnection can occur has shown that reconnection is favoured in regions away from the subsolar point and at higher latitudes with a range of local times [*Desroche et al.*, 2013]. This is supported by independent global MHD simulations [*Fukazawa et al.*, 2007].

Although no FTE signatures have been reported at Saturn, there is observational evidence for reconnection. Entry of magnetosheath plasma into Saturn's magnetospheric cusp via 'bursty' or 'pulsed' reconnection has been observed [*Jasinski et al.*, 2014; *Arridge et al.*, 2016]. In situ observations of heated electrons near the dawnside magnetopause suggest the occurrence of reconnection [*McAndrews et al.*, 2008]. Poleward moving bifurcations in the aurora are evidence for magnetopause reconnection [e.g. *Radioti et al.*, 2011, 2013]. Bursts of magnetospheric electrons on reconnected field lines in the magnetosheath coincident with auroral reconnection signatures have also been reported [*Badman et al.*, 2013]. Similarly, *Fuselier et al.* [2014] presented 18 events where magnetospheric

Author Manuscript

This article is protected by copyright. All rights reserved.

electrons present in the magnetosheath show evidence for reconnection and the associated magnetic shear angles were estimated to be >104°.

No comprehensive search was undertaken to find FTEs in this report. Here we investigate a single dayside magnetopause crossing on February 2nd 2007 at Saturn by the Cassini spacecraft. This crossing contains evidence that an FTE-type flux rope was observed in a region of newly opened flux tubes adjacent to the magnetopause. First, we present a brief summary of the instrumentation used, and Cassini's trajectory. Secondly, we present an overview of the observations, including minimum variance analysis of the data and a comparison to a flux rope model. Finally, we discuss the implications of these new observations for Saturn's magnetosphere.

2. Instrumentation

In situ electron and proton observations are presented from the Low-Energy-Magnetospheric-Measurement-System (LEMMS) [*Krimigis et al.*, 2004], and the Electron and Ion-Mass Spectrometers (ELS and IMS respectively) from the Cassini-Plasma-Spectrometer (CAPS) [*Young et al.*, 2004].

The Magnetometer (MAG) data are presented in the Kronographic-Radial-Theta-Phi (KRTP) coordinate system (spherical polar coordinates) which is spacecraft-centered for the magnetic field and planet-centered for the position of the spacecraft [*Dougherty et al.*, 2004]. The radial ($\boldsymbol{R}$) vector is directed in the planet-spacecraft direction, the azimuthal vector ($\boldsymbol{\phi}$) is positive in the direction of Saturn's rotation, and $\boldsymbol{\theta}$ completes the right-hand set ($\boldsymbol{\theta}=\boldsymbol{R}\times\phi$) and is in the colatitudinal direction, positive southwards. For readers who are used to a cartesian coordinate system, due to the location of the spacecraft during this

Author Manuscript

This article is protected by copyright. All rights reserved.

interval being close to the subsolar point, the KRTP vectors at low-latitudes are directed similarly to a Solar-Magnetospheric system, with $\boldsymbol{R}$ approximately in the $\boldsymbol{X}$ (i.e. planet-Sun) direction, $\boldsymbol{\theta}$ approximately in the -$\boldsymbol{Z}$ direction (i.e. southwards) and $\boldsymbol{\phi}$ approximately in the duskward direction (i.e. $\boldsymbol{Y}$).

3. Observations

3.1. Spacecraft Trajectory

The highly inclined trajectory of Cassini (Figure 2), shows it passed over the southern pole on the dawnward side of the planet, crossed near the subsolar point of the bow shock, followed by passing over the northern pole on the duskward side. The average location of the magnetopause at the subsolar position has a bimodal distribution at $\sim$22 R_S and $\sim$27 R_S [*Achilleos et al.*, 2008]. Therefore the magnetopause crossing at $\sim$17.3 R_S during this interval shows that Saturn's magnetosphere was significantly compressed. This is supported by results from a solar wind propagation model [*Zieger and Hansen*, 2008] which forecast the arrival of a significant increase in the dynamic pressure at this time (see the online supporting material, 'OSM'), which compressed the magnetosphere.

Earlier in the trajectory (and on the same day as the event we present) whilst in the high-latitude magnetosphere, Cassini encountered the cusp where magnetosheath plasma was observed [*Arridge et al.*, 2016]. During our event, Cassini was travelling in an equatorward direction, and was located at a radial distance of $\sim$17.3 R_S from the planet, a latitude of $\sim$-24° and a local time of 12:50.

This article is protected by copyright. All rights reserved.

Author Manuscript

3.2. Overview

At 23:22−23:33 UT Cassini was located in the magnetosphere where the magnetic field was strongly dipolar (i.e. predominantly in the B_θ direction; Figure 1d). Whilst in the magnetosphere, five TCRs were observed (shaded red). TCRs are observed when the spacecraft passes near, but does not penetrate a flux rope. Instead, a region of compressed magnetic field lines is observed which drapes around the flux rope (Figure 1a). Hence a TCR is a two-dimensional compression wave which passes over the spacecraft. They are observed via rotations in the magnetic field in a single plane, coincident with an increase in magnitude (Figure 1f) [e.g. *Zhang et al.*, 2010; *Slavin et al.*, 2012]. The first two TCRs had bipolar signatures in the radial direction, whilst all had increases in the colatitudinal direction and in magnitude.

An overview of the observations is shown in Figure 3. Whilst in the magnetosphere, energetic electrons, $\sim 10^2$ to 10^4 eV, were observed (panels a-c), and the electron number density was low (d). At ∼23:33 UT Cassini entered a boundary layer. The drop in observed ion counts (Figure 3e, 23:33−23:42 UT) just after the vertical blue line occurred because the IMS field-of-view (FOV) moved out of the peak ion flow direction. At ∼23:44 UT, Cassini entered the magnetosheath where electrons with lower energies, ~ 10 to 10^3 eV and the highest electron number densities, ~ 1.5 cm^{-3} (both characteristic of the magnetosheath), were observed. The electron number density was approximately an order of magnitude higher than the statistical average ion number density in the magnetosheath [*Sergis et al.*, 2013], consistent with the interpretation that the magnetosphere was being compressed by an increase in the solar wind dynamic pressure. There was a very large

This article is protected by copyright. All rights reserved.

Author Manuscript

decrease in magnetic field magnitude including a rotation across the boundary. At ∼23:53 UT, Cassini crossed the bow shock and entered the solar wind.

The region between the magnetosphere and magnetosheath is interpreted to be a region of open flux (grey shading in Figure 3) which had just undergone reconnection (with an embedded FTE-type flux rope). This is supported by the following observations. Firstly, the magnetic field magnitude decreased from ∼7 nT (in the magnetosphere) to ∼4 nT; also the magnetic field direction was observed to rotate from a magnetospheric dipolar configuration (positive $\boldsymbol{\theta}$) to an oppositely orientated direction, including an increase (and a rotation) in the azimuthal direction, $\boldsymbol{\phi}$. Therefore the spacecraft was no longer traversing closed field lines as the field was no longer in a direction consistent with the magnetospheric magnetic field. Secondly, the plasma instruments observed magnetosheath-like plasma throughout, as well as magnetospheric plasma present in the first half of the open region. This shows that the spacecraft observed a mixed plasma population from both adjacent regions. The magnetosheath-like plasma (higher in energy due to energisation from reconnection and lower in density than the adjacent magnetsheath) is similar to plasma observed in Saturn's cusp [*Jasinski et al.*, 2014; *Arridge et al.*, 2016] which is also located on open field lines. At the beginning of this open region at ∼23:34 UT an increase in the magnetic field magnitude was observed including a bipolar signature in the radial direction which we have identified to be an FTE (blue line). A comparison of the electron energy-distributions between the different regions can be seen in the OSM.

Author Manuscript

This article is protected by copyright. All rights reserved.

3.3. Minimum Variance Analysis

Minimum variance analysis (MVA) was performed on the FTE-type flux rope and the boundary crossing between the open region and magnetosphere, to further characterise these events and understand their magnetic structure. MVA can be used to determine the orientation of the flux rope axis by transforming the magnetic field data into a new orthogonal coordinate system with unit vectors in the maximum, minimum and intermediate variance directions [*Sonnerup and Cahill*, 1967]. This method has been used extensively at various planetary magnetospheres to analyse magnetic structures [e.g. *Huddleston et al.*, 1997; *Eastwood et al.*, 2002; *Knetter et al.*, 2004; *Steed et al.*, 2011; *Jackman et al.*, 2014; *Slavin et al.*, 2014]. If the spacecraft passed near the center of the FTE, then the magnetic field in the minimum direction will be small (or approach zero) throughout the flux rope observation. If the flux rope is force-free then the intermediate vector corresponds to the axis [e.g. *Xiao et al.*, 2004] of the FTE (Figure 1b).

MVA from the boundary crossing between the magnetosphere and the open region at 23:32:09–23:33:03 UT resulted in a minimum variance direction (in KRTP) of (0.98, -0.13, -0.14), predominantly in the radial direction. This is very similar to the normal direction calculated from the *Kanani et al.* [2010] magnetopause model of (0.98, 0.18, -0.09), showing that the boundary is similarly aligned to the magnetopause.

The FTE observation in the magnetopause normal (LMN) coordinate system can be seen in the OSM. Figure 4 shows the MVA results for the FTE with a model flux rope shown in blue (discussed below). The calculated eigenvector ($\boldsymbol{x}$) for each direction is shown in KRTP coordinates, as well as its corresponding eigenvalue (λ). The eigenvalue ratios

This article is protected by copyright. All rights reserved.

were greater than four and so the vectors were well determined [*Sonnerup and Cahill*, 1967; *Collier and Lepping*, 1996]. The flux rope had a very strong bipolar signature in the maximum direction, which is the basic flux rope signature. B_{min} ~2 nT, is not zero, so the spacecraft did not pass through the centre of the flux rope, but it did penetrate deeply into the structure. The minimum variance vector (predominantly in the radial and latitudinal directions) shows the direction the spacecraft passed through the flux rope (in its rest frame). In reality, the spacecraft speed is negligible (~7 km/s) in comparison to the flux rope (hundreds of km/s) and is considered stationary, so the flux rope passed over the spacecraft in a planetward and southward direction, consistent with a multiple reconnection x-line located equatorward of Cassini. This motion of the FTE-type flux rope is supported by the angular distribution of the ions which showed bulk flow to be in a similar direction.

3.4. Flux Rope Modeling

The flux rope was compared to a force-free flux rope model first put forward by *Lundquist* [1950] and developed by *Lepping et al.* [1990, 1995]. In a force-free magnetic field, the current density **J** is parallel to the magnetic field **B** (i.e. **J**×**B**=0). Therefore:

$$\nabla \times \mathbf{B} = \mathbf{J} = \alpha \mathbf{B} \tag{1}$$

where α is a constant proportionality factor and determined to be 2.405 so that the magnetic field is purely axial and tangential at the centre and the edge of the flux rope, respectively (Figure 1b). Taking the curl of both sides gives:

This article is protected by copyright. All rights reserved.

Author Manuscript

$$\nabla^2 \mathbf{B} = -\alpha^2 \mathbf{B} \tag{2}$$

The solution in cylindrical coordinates to Equation 2 was shown to be a function of the Bessel functions of the first kind [*Lundquist*, 1950]:

$$B_A = B_0 J_0\left(\frac{\alpha r}{R_{FR}}\right) \qquad B_T = H B_0 J_1\left(\frac{\alpha r}{R_{FR}}\right) \qquad B_R = 0 \tag{3}$$

where H is the helicity of the structure and is equal to ± 1. B_0 is the magnetic field magnitude at the centre of the rope. r/R_{FR} is the impact factor to flux rope radius (R_{FR}) ratio and represents the distance of closest approach to the centre of the FTE. J_0, and J_1 are the zeroth and first-order Bessel functions. B_0 and r/R_{FR} are unknowns, and estimated in this process. The MVA intermediate vector was used to form the axial direction of the FTE-type flux rope. The maximum and minimum directions formed the tangential direction of the flux rope, whereby the minimum eigenvector formed the trajectory direction through the FTE. The model was fit using a least-squares minimisation algorithm for r/R_{FR} in MVA coordinates. The value of B_0 was scaled accordingly after this process (see *Slavin et al.* [2003] for more details).

The value of the best-fit impact factor was $\sim$0.3 R_{FR}, with a B_0 of $\sim$7 nT. Figure 4c-e shows a comparison of the flux rope model (in blue) to the data. B_{min} was very well modeled throughout the FTE, whilst most of B_{int} was well modeled at the centre. The bipolar signature of B_{max} was also found to match the observations.

The magnetic flux content (Φ) of the FTE-type flux rope was calculated using:

Author Manuscript

This article is protected by copyright. All rights reserved.

$$\Phi = \frac{2\pi}{\alpha} B_0 R_{FR}^2 J_1(\alpha) \tag{4}$$

To calculate flux rope radius, the transit time and velocity of the flux rope passing through the spacecraft (calculated from the CAPS-IMS ion observations) were used. The restricted FOV of IMS is not amenable to the standard moment integration techniques [e.g. *Thomsen et al.*, 2010; *Wilson et al.*, 2008] as they require the instrument to see the peak flow to calculate the flow velocity. However, the peak flux can be constrained to anodes 5, 6 and 7 of IMS. Ion distributions can be well modeled as the sum of two co-moving proton distributions with different temperatures, a hot and cold distribution, with temperatures of 1 keV and 100 eV, respectively [*Richardson*, 1987]. The model distribution consisted of the sum of two drifting-Maxwellians (one each for the hot and cold proton distributions) and were fitted with non-linear least squares. From the model, the peak flow was found to be located 0-20° outside the FOV of IMS (flowing southward). The resulting ion flow speeds were calculated to be 473±9 to 540±6 km/s, where the uncertainty in each measurement comes from the uncertainties from the non-linear fit and the range originates in the assumed angle between the sensors and the ion flow direction.

Using the lower and upper estimates of the velocity (mentioned above) the size of the FTE is approximated to be ∼6500 and ∼7400 km (∼0.1 R_S). However, there are errors associated with the force-free-fitting technique including the assumption of a force-free cylindrically-shaped structure. In reality, non-negligible plasma gradients will be present in any FTE, and FTEs will not be completely cyclindrical. This will make the assumptions not completely valid, because flux ropes are usually observed whilst in the

Author Manuscript

This article is protected by copyright. All rights reserved.

process of evolving to become near-force-free [*Kivelson et al.*, 1993; *Zhang et al.*, 2010]. Errors associated with the selection of the FTE time duration will have the biggest effect on the calculated size of the flux rope and Φ, whilst the uncertainty on the impact factor is an order of magnitude smaller. The start-stop times were chosen to coincide with the peaks in the bipolar signature, but an increase or decrease of three seconds would result in a flux rope radius value to lie between $\sim$4600 and $\sim$8300 km, and a magnetic flux content between $\sim$0.2 and $\sim$0.8 MWb.

4. Discussion and Conclusions

We have presented the first detection of an FTE-type flux rope at Saturn's dayside magnetopause. The Cassini spacecraft passed from the magnetosphere, where it observed four TCRs and then passed into an open flux region where energised magnetosheath plasma was observed as well as the FTE-type flux rope. The observation of TCRs in the magnetosphere, and the flux rope in the open region all support the interpretation that Cassini passed from the magnetosphere onto newly reconnected open magnetic field lines, which are adjacent to the magnetopause and therefore would map at higher latitudes to the cusp. Cassini then crossed into the magnetosheath, where the plasma increased in density, before finally traversing the bow shock and into the solar wind.

An estimation of the plasma β yielded values of $\sim$1, $\sim$5 and $\sim$19 for the magnetosphere, the open region and the magnetosheath, respectively. These calculations were made by adding the plasma pressures from the MIMI and CAPS instruments [*Sergis et al.*, 2009; *Thomsen et al.*, 2010], for the entire open region and magnetosheath, and for nine minutes within the magnetosphere (23:20−23:29). The difference in β between the magnetosphere

This article is protected by copyright. All rights reserved.

and the open region is quite low in comparison to some magnetopause crossings at Saturn analysed by *Masters et al.* [2012].

However the β in the observed magnetosheath (adjacent to the open region) is quite high. The assumption that the conditions that formed the open region were similar to the observed magnetosheath, would require a high magnetic shear for magnetic reconnection. Either the magnetic shear that prompted reconnection was very high or the β-dependence models [*Swisdak et al.*, 2010; *Masters et al.*, 2012] do not provide a complete picture of the conditions required for reconnection onset. However, we do know reconnection had occurred and formed the observed FTE and open region, and further analysis of the reconnection conditions are beyond the scope of this paper.

MVA was performed on the flux rope magnetic field measurements. The axis of the FTE (i.e. the intermediate variance direction) was found to be predominantly in the azimuthal direction (i.e. east-west), and it was found to be moving southward. Both of these characteristics are consistent with the high-shear, multiple x-line model for FTE generation [*Lee and Fu*, 1985; *Raeder*, 2006], which is well supported by observations at Earth [e.g. *Fear et al.*, 2008].

A force-free cylindrical constant-α flux rope model was fit to the FTE magnetic field measurements. The result shows that Cassini's closest approach to the flux rope core was $\sim$0.3 R_{FR}, and the core field strength was $\sim$7 nT. Using the observed ion flow velocities, the flux content of the FTE was estimated to be between $\sim$0.2 and $\sim$0.8 MWb. Terrestrial FTEs have been observed to contain similar amounts of magnetic flux, e.g., 0.3 MWb [*Lui et al.*, 2008] and 0.4 MWb [*Zhang et al.*, 2008].

This article is protected by copyright. All rights reserved.

Author Manuscript

Assuming the five observed TCRs in this event are attributed to FTEs, would give an FTE occurrence of ∼2 minutes (six FTEs are observed in nine minutes), which is less than the ∼8 minutes and more than the ∼8 seconds observed at Earth and Mercury respectively [*Rijnbeek et al.*, 1984; *Slavin et al.*, 2012]. Six FTEs in 9 minutes, would result in a reconnection voltage of ∼2-9 kV (attributed solely to FTE generation).

In a comprehensive auroral study, *Badman et al.* [2013] estimated reconnection voltages of ∼30-200 kV, whilst *McAndrews et al.* [2008] reported ∼48 kV and *Jackman et al.* [2004] estimated voltages of ∼10-400 kV . Modeling of the reconnection voltage at Saturn revealed an average of ∼40 kV, with an upper estimate of ∼100 kV [*Masters*, 2015]. The event presented here is during a magnetospheric compression, and the upper value from *Masters* [2015] and *Badman et al.* [2013] are more likely for our interval. Therefore it could conceivably be estimated (assuming six FTEs are generated every nine minutes, and the associated resulting reconnection voltage is ∼2-9 kV) that FTEs at Saturn contribute ∼1-9% to the opening of flux during solar wind compressions. However our observations are local to Cassini, and these estimates could be conservative because more FTEs might be generated elsewhere along Saturn's huge magnetopause, that are not sampled on Cassini's trajectory. Although this is the first reported event, this FTE may not be representative of FTEs at Saturn and a statistical survey will provide a better understanding of the variability in flux opened in FTEs.

It is not possible from this study to determine whether the flux rope reconnection voltage is the same during quiescent solar wind conditions. It is more than likely that FTE-type flux rope generation is negligible at Saturn when the overall dayside reconnection rate

Author Manuscript

This article is protected by copyright. All rights reserved.

is very low, with fewer multiple x-lines occurring during less stressed magnetospheric conditions. This would explain the general lack of FTE observations to date. However we have shown that there are events at the Saturnian magnetopause where reconnection occurs in an Earth-like manner and an FTE can be formed. A re-examination of the magnetopause crossings should be undertaken to search for flux rope signatures in the data.

Acknowledgments. We thank the MSSL CAPS operations team, L. K. Gilbert, G. R. Lewis and N. Shane for support in calibration and data display. JMJ was supported by STFC Studentship ST/J500914/1 whilst at MSSL−UCL. CSA is supported by a Royal Society University Research Fellowship. JHW was supported by a CAPS Cassini contract from NASA JPL. We acknowledge support via the MSSL consolidated grant from STFC, as well as travel support from the Royal Astronomical Society. This work was also supported by the NASA Discovery Data Analysis Program under grant NNX15AK88G. All the data for this study can be found at NASA's planetary data system (https://pds.jpl.nasa.gov).

References

Arridge, C. S., N. Achilleos, M. K. Dougherty, K. K. Khurana, and C. T. Russell (2006), Modeling the size and shape of Saturn's magnetopause with variable dynamic pressure, *J. Geophys. Res., (Space Physics)*, *111*, A11227, doi:10.1029/2005JA011574.

Arridge, C., et al. (2016), Cassini observations of saturn's southern polar cusp, *Journal of Geophysical Research: Space Physics*, doi:10.1002/2015JA021957, 2015JA021957.

Author Manuscript

This article is protected by copyright. All rights reserved.

Achilleos, N., C. S. Arridge, C. Bertucci, C. M. Jackman, M. K. Dougherty, K. K. Khurana, and C. T. Russell (2008), Large-scale dynamics of saturn's magnetopause: Observations by cassini, *J. of Geophys. Res.*, *113*(A11), doi:10.1029/2008JA013265.

Aubry, M. P., C. T. Russell, and M. G. Kivelson (1970), Inward motion of the magnetopause before a substorm, *Journal of Geophysical Research*, *75*(34), 7018–7031, doi:10.1029/JA075i034p07018.

Badman, S. V., A. Masters, H. Hasegawa, M. Fujimoto, A. Radioti, D. Grodent, N. Sergis, M. K. Dougherty, and A. J. Coates (2013), Bursty magnetic reconnection at Saturn's magnetopause, *Geophys. Res. Lett.*, , *40*, 1027–1031, doi:10.1002/grl.50199.

Brain, D. A., A. H. Baker, J. Briggs, J. P. Eastwood, J. S. Halekas, and T.-D. Phan (2010), Episodic detachment of martian crustal magnetic fields leading to bulk atmospheric plasma escape, *Geophysical Research Letters*, *37*(14), doi:10.1029/2010GL043916, l14108.

Burton, R. K., R. L. McPherron, and C. T. Russell (1975), The terrestrial magnetosphere - A half-wave rectifier of the interplanetary electric field, *Science*, *189*, 717, doi:10.1126/science.189.4204.717.

Collier, M., and R. Lepping (1996), Jovian magnetopause breathing, *Planetary and Space Science*, *44*(3), 187 – 197, doi:http://dx.doi.org/10.1016/0032-0633(95)00117-4.

Cowley, S., and C. Owen (1989), A simple illustrative model of open flux tube motion over the dayside magnetopause, *Planetary and Space Science*, *37*(11), 1461 – 1475, doi:http://dx.doi.org/10.1016/0032-0633(89)90116-5.

Author Manuscript

This article is protected by copyright. All rights reserved.

Desroche, M., F. Bagenal, P. A. Delamere, and N. Erkaev (2013), Conditions at the magnetopause of Saturn and implications for the solar wind interaction, *Journal of Geophysical Research (Space Physics)*, *118*, 3087–3095, doi:10.1002/jgra.50294.

DiBraccio, G. A., et al. (2013), Messenger observations of magnetopause structure and dynamics at mercury, *Journal of Geophysical Research: Space Physics*, *118*(3), 997–1008, doi:10.1002/jgra.50123.

Dougherty, M. K., S. Kellock, D. J. Southwood, A. Balogh, E. J. Smith, B. T. Tsurutani, B. Gerlach, K.-H. Glassmeier, F. Gleim, C. T. Russell, G. Erdos, F. M. Neubauer, and S. W. H. Cowley (2004), The Cassini Magnetic Field Investigation, *SSR*, *114*, 331–383, doi:10.1007/s11214-004-1432-2.

Eastwood, J. P., A. Balogh, M. W. Dunlop, and C. W. Smith (2002), Cluster observations of the heliospheric current sheet and an associated magnetic flux rope and comparisons with ace, *Journal of Geophysical Research: Space Physics*, *107*(A11), SSH 9–1–SSH 9–9, doi:10.1029/2001JA009158, 1365.

Elphic, R. C., C. T. Russell, J. A. Slavin, and L. H. Brace (1980), Observations of the dayside ionopause and ionosphere of venus, *Journal of Geophysical Research: Space Physics*, *85*(A13), 7679–7696, doi:10.1029/JA085iA13p07679.

Fear, R. C., A. N. Fazakerley, C. J. Owen, and E. A. Lucek (2005), A survey of flux transfer events observed by Cluster during strongly northward IMF, *Geophys. Res. Lett.,* , *32*, L18105, doi:10.1029/2005GL023811.

Fear, R. C., S. E. Milan, A. N. Fazakerley, E. A. Lucek, S. W. H. Cowley, and I. Dandouras (2008), The azimuthal extent of three flux transfer events, *Annales Geophysicae*, *26*,

This article is protected by copyright. All rights reserved.

2353–2369, doi:10.5194/angeo-26-2353-2008.

Fu, Z. F., and L. C. Lee (1985), Simulation of multiple x-line reconnection at the dayside magnetopause, *Geophysical Research Letters*, *12*(5), 291–294, doi: 10.1029/GL012i005p00291.

Fukazawa, K., S.-i. Ogi, T. Ogino, and R. J. Walker (2007), Magnetospheric convection at Saturn as a function of IMF BZ, *Geophys. Res. Lett.,* , *34*, 1105, doi: 10.1029/2006GL028373.

Fuselier, S. A., R. Frahm, W. S. Lewis, A. Masters, J. Mukherjee, S. M. Petrinec, and I. J. Sillanpaa (2014), The location of magnetic reconnection at saturn's magnetopause: A comparison with earth, *Journal of Geophysical Research: Space Physics*, *119*(4), 2563–2578, doi:10.1002/2013JA019684, 2013JA019684.

Gershman, D. J., J. A. Slavin, J. M. Raines, T. H. Zurbuchen, B. J. Anderson, H. Korth, D. N. Baker, and S. C. Solomon (2013), Magnetic flux pileup and plasma depletion in mercury's subsolar magnetosheath, *Journal of Geophysical Research: Space Physics*, *118*(11), 7181–7199, doi:10.1002/2013JA019244, 2013JA019244.

Huddleston, D. E., C. T. Russell, G. Le, and A. Szabo (1997), Magnetopause structure and the role of reconnection at the outer planets, *J. Geophys. Res.,* , *102*, 24,289–24,004, doi:10.1029/97JA02416.

Imber, S. M., J. A. Slavin, S. A. Boardsen, B. J. Anderson, H. Korth, R. L. McNutt, and S. C. Solomon (2014), Messenger observations of large dayside flux transfer events: Do they drive mercury's substorm cycle?, *Journal of Geophysical Research: Space Physics*, *119*(7), 5613–5623, doi:10.1002/2014JA019884, 2014JA019884.

Author Manuscript

This article is protected by copyright. All rights reserved.

Jackman, C. M., N. Achilleos, E. J. Bunce, S. W. H. Cowley, M. K. Dougherty, G. H. Jones, S. E. Milan, and E. J. Smith (2004), Interplanetary magnetic field at ∼9 AU during the declining phase of the solar cycle and its implications for Saturn's magnetospheric dynamics, *Journal of Geophysical Research (Space Physics)*, *109*, A11203, doi:10.1029/2004JA010614.

Jackman, C. M., et al. (2014), Saturn's dynamic magnetotail: A comprehensive magnetic field and plasma survey of plasmoids and traveling compression regions and their role in global magnetospheric dynamics, *Journal of Geophysical Research: Space Physics*, *119*(7), 5465–5494, doi:10.1002/2013JA019388, 2013JA019388.

Jasinski, J. M., C. S. Arridge, L. Lamy, J. S. Leisner, M. F. Thomsen, D. G. Mitchell, A. J. Coates, A. Radioti, G. H. Jones, E. Roussos, N. Krupp, D. Grodent, M. K. Dougherty, and J. H. Waite (2014), Cusp observation at Saturn's high-latitude magnetosphere by the Cassini spacecraft, *Geophys. Res. Lett.*, *41*, 1382–1388, doi:10.1002/2014GL059319.

Kanani, S. J., C. S. Arridge, G. H. Jones, A. N. Fazakerley, H. J. McAndrews, N. Sergis, S. M. Krimigis, M. K. Dougherty, A. J. Coates, D. T. Young, K. C. Hansen, and N. Krupp (2010), A new form of Saturn's magnetopause using a dynamic pressure balance model, based on in situ, multi-instrument Cassini measurements, *J. Geophys. Res.*, *115*, A06207, doi:10.1029/2009JA014262.

Khurana, K. K., et al. (2006), A Model of Saturn's Magnetospheric Field Based on Latest Cassini Observations.

Kivelson, M. G., et al. (1993), The galileo earth encounter: Magnetometer and allied measurements, *Journal of Geophysical Research: Space Physics*, *98*(A7), 11,299–11,318,

This article is protected by copyright. All rights reserved.

doi:10.1029/92JA03001.

Kivelson, M. G., and D. J. Southwood (2003), First evidence of {IMF} control of jovian magnetospheric boundary locations: Cassini and galileo magnetic field measurements compared, *Planetary and Space Science*, *51*(13), 891 – 898, doi: http://dx.doi.org/10.1016/S0032-0633(03)00075-8.

Knetter, T., F. M. Neubauer, T. Horbury, and A. Balogh (2004), Four-point discontinuity observations using cluster magnetic field data: A statistical survey, *Journal of Geophysical Research: Space Physics*, *109*(A6), doi:10.1029/2003JA010099, a06102.

Krimigis, S. M., D. G. Mitchell, D. C. Hamilton, S. Livi, J. Dandouras, S. Jaskulek, T. P. Armstrong, J. D. Boldt, A. F. Cheng, G. Gloeckler, J. R. Hayes, K. C. Hsieh, W.-H. Ip, E. P. Keath, E. Kirsch, N. Krupp, L. J. Lanzerotti, R. Lundgren, B. H. Mauk, R. W. McEntire, E. C. Roelof, C. E. Schlemm, B. E. Tossman, B. Wilken, and D. J. Williams (2004), Magnetosphere Imaging Instrument (MIMI) on the Cassini Mission to Saturn/Titan, *Space Science Reviews*, *114*, 233–329, doi:10.1007/s11214-004-1410-8.

Lai, H. R., H. Y. Wei, C. T. Russell, C. S. Arridge, and M. K. Dougherty (2012), Reconnection at the magnetopause of Saturn: Perspective from FTE occurrence and magnetosphere size, *Journal of Geophysical Research (Space Physics)*, *117*, A05222, doi: 10.1029/2011JA017263.

Lee, L. C., and Z. F. Fu (1985), A theory of magnetic flux transfer at the earth's magnetopause, *Geophysical Research Letters*, *12*(2), 105–108, doi:10.1029/GL012i002p00105.

Lepping, R. P., J. A. Jones, and L. F. Burlaga (1990), Magnetic field structure of interplanetary magnetic clouds at 1 au, *Journal of Geophysical Research: Space Physics*,

Author Manuscript

This article is protected by copyright. All rights reserved.

95(A8), 11,957–11,965, doi:10.1029/JA095iA08p11957.

Lepping, R. P., D. H. Fairfield, J. Jones, L. A. Frank, W. R. Paterson, S. Kokubun, and T. Yamamoto (1995), Cross-tail magnetic flux ropes as observed by the GEOTAIL spacecraft, *Geophys. Res. Lett.,* , *22*, 1193–1196, doi:10.1029/95GL01114.

Lui, A. T. Y., D. G. Sibeck, T. Phan, J. P. McFadden, V. Angelopoulos, and K.-H. Glassmeier (2008), Reconstruction of a flux transfer event based on observations from five themis satellites, *Journal of Geophysical Research: Space Physics*, *113*(A1), doi:10.1029/2008JA013189, a00C01.

Lundquist, S. (1950), Magneto-hydrostatic fields, *Arkiv for fysik*, *2*(4), 361–365.

McAndrews, H. J., C. J. Owen, M. F. Thomsen, B. Lavraud, A. J. Coates, M. K. Dougherty, and D. T. Young (2008), Evidence for reconnection at Saturn's magnetopause, *Journal of Geophysical Research (Space Physics)*, *113*, A04210, doi:10.1029/2007JA012581.

Masters, A., D. G. Mitchell, A. J. Coates, and M. K. Dougherty (2011a), Saturn's low-latitude boundary layer: 1. Properties and variability, *Journal of Geophysical Research (Space Physics)*, *116*, A06210, doi:10.1029/2010JA016421.

Masters, A., A. P. Walsh, A. N. Fazakerley, A. J. Coates, and M. K. Dougherty (2011b), Saturn's low-latitude boundary layer: 2. Electron structure, *Journal of Geophysical Research (Space Physics)*, *116*, A06211, doi:10.1029/2010JA016422.

Masters, A., et al. (2012), The importance of plasma β conditions for magnetic reconnection at Saturn's magnetopause, *Geophys. Res. Lett.,* , *39*, L08103, doi:10.1029/2012GL051372.

Author Manuscript

This article is protected by copyright. All rights reserved.

Masters, A. (2015), The dayside reconnection voltage applied to saturn's magnetosphere, *Geophysical Research Letters*, *42*(8), 2577–2585, doi:10.1002/2015GL063361, 2015GL063361.

Mozer, F. S., and A. Retinò (2007), Quantitative estimates of magnetic field reconnection properties from electric and magnetic field measurements, *Journal of Geophysical Research (Space Physics)*, *112*, A10206, doi:10.1029/2007JA012406.

Owen, C. J., et al. (2008), Cluster observations of "crater" flux transfer events at the dayside high-latitude magnetopause, *Journal of Geophysical Research (Space Physics)*, *113*, A07S04, doi:10.1029/2007JA012701.

Quest, K. B., and F. V. Coroniti (1981), Linear theory of tearing in a high-beta plasma, *J. Geophys. Res.,* , *86*, 3299–3305, doi:10.1029/JA086iA05p03299.

Radioti, A., D. Grodent, J.-C. Gérard, S. E. Milan, B. Bonfond, J. Gustin, and W. Pryor (2011), Bifurcations of the main auroral ring at Saturn: ionospheric signatures of consecutive reconnection events at the magnetopause, *Journal of Geophysical Research (Space Physics)*, *116*, A11209, doi:10.1029/2011JA016661.

Radioti, A., D. Grodent, J.-C. Gérard, B. Bonfond, J. Gustin, W. Pryor, J. M. Jasinski, and C. S. Arridge (2013), Auroral signatures of multiple magnetopause reconnection at Saturn, *Geophys. Res. Lett.,* , *40*, 4498–4502, doi:10.1002/grl.50889.

Raeder, J. (2006), Flux transfer events: 1. generation mechanism for strong southward imf, *Annales Geophysicae*, *24*(1), 381–392, doi:10.5194/angeo-24-381-2006.

Richardson, J. D. (1987), Ion distributions in the dayside magnetosheaths of jupiter and saturn, *Journal of Geophysical Research: Space Physics*, *92*(A6), 6133–6140, doi:

Author Manuscript

This article is protected by copyright. All rights reserved.

10.1029/JA092iA06p06133.

Rijnbeek, R. P., S. W. H. Cowley, D. J. Southwood, and C. T. Russell (1984), A survey of dayside flux transfer events observed by isee 1 and 2 magnetometers, *Journal of Geophysical Research: Space Physics*, *89*(A2), 786–800, doi:10.1029/JA089iA02p00786.

Russell, C. T., and R. C. Elphic (1978), Initial ISEE magnetometer results - Magnetopause observations, *Space Science Reviews*, *22*, 681–715, doi:10.1007/BF00212619.

Russell, C. T., and R. C. Elphic (1979), Isee observations of flux transfer events at the dayside magnetopause, *Geophysical Research Letters*, *6*(1), 33–36, doi: 10.1029/GL006i001p00033.

Russell, C. T., and R. J. Walker (1985), Flux transfer events at mercury, *Journal of Geophysical Research: Space Physics*, *90*(A11), 11,067–11,074, doi: 10.1029/JA090iA11p11067.

Russell, C. (1995), A study of flux transfer events at different planets, *Advances in Space Research*, *16*(4), 159 – 163, doi:http://dx.doi.org/10.1016/0273-1177(95)00224-3, comparative Studies of Magnetospheric Phenomena.

Šafránková, J., Z. Němeček, L. Přech, J. Šimůnek, D. Sibeck, and J.-A. Sauvaud (2007), Variations of the flank LLBL thickness as response to the solar wind dynamic pressure and IMF orientation, *J. of Geophys. Res.*, *112*, A07201, doi:10.1029/2006JA011889.

Scholer, M. (1988), Magnetic flux transfer at the magnetopause based on single x line bursty reconnection, *Geophysical Research Letters*, *15*(4), 291–294, doi: 10.1029/GL015i004p00291.

Author Manuscript

This article is protected by copyright. All rights reserved.

Scurry, L., C. T. Russell, and J. T. Gosling (1994), Geomagnetic activity and the beta dependence of the dayside reconnection rate, *Journal of Geophysical Research: Space Physics*, *99*(A8), 14,811–14,814, doi:10.1029/94JA00794.

Sergis, N., S. M. Krimigis, D. G. Mitchell, D. C. Hamilton, N. Krupp, B. H. Mauk, E. C. Roelof, and M. K. Dougherty (2009), Energetic particle pressure in saturn's magnetosphere measured with the magnetospheric imaging instrument on cassini, *Journal of Geophysical Research: Space Physics*, *114*(A2), doi:10.1029/2008JA013774, a02214.

Sergis, N., C. M. Jackman, A. Masters, S. M. Krimigis, M. F. Thomsen, D. C. Hamilton, D. G. Mitchell, M. K. Dougherty, and A. J. Coates (2013), Particle and magnetic field properties of the saturnian magnetosheath: Presence and upstream escape of hot magnetospheric plasma, *Journal of Geophysical Research: Space Physics*, *118*(4), 1620–1634, doi:10.1002/jgra.50164.

Slavin, J. A., R. E. Holzer, J. R. Spreiter, and S. S. Stahara (1984), Planetary Mach cones - Theory and observation, *J. Geophys. Res.,* , *89*, 2708–2714, doi:10.1029/JA089iA05p02708.

Slavin, J. A., et al. (2003), Geotail observations of magnetic flux ropes in the plasma sheet, *Journal of Geophysical Research: Space Physics*, *108*(A1), SMP 10–1–SMP 10–18, doi:10.1029/2002JA009557, 1015.

Slavin, J. A., et al. (2009), MESSENGER Observations of Magnetic Reconnection in Mercury's Magnetosphere, *Science*, *324*, 606–, doi:10.1126/science.1172011.

Slavin, J. A., et al. (2010), MESSENGER observations of large flux transfer events at Mercury, *Geophys. Res. Lett.,* , *37*, L02105, doi:10.1029/2009GL041485.

This article is protected by copyright. All rights reserved.

Slavin, J. A., et al. (2012), MESSENGER observations of a flux-transfer-event shower at Mercury, *Journal of Geophysical Research (Space Physics)*, *117*, A00M06, doi:10.1029/2012JA017926.

Slavin, J. A., et al. (2014), MESSENGER observations of Mercury's dayside magnetosphere under extreme solar wind conditions, *Journal of Geophysical Research (Space Physics)*, *119*, 8087–8116, doi:10.1002/2014JA020319.

Sonnerup, B. U. ., and L. J. Cahill (1967), Magnetopause structure and attitude from explorer 12 observations, *Journal of Geophysical Research*, *72*(1), 171–183, doi:10.1029/JZ072i001p00171.

Southwood, D., C. Farrugia, and M. Saunders (1988), What are flux transfer events?, *Planetary and Space Science*, *36*(5), 503 – 508, doi:http://dx.doi.org/10.1016/0032-0633(88)90109-2.

Steed, K., C. J. Owen, P. Dmoulin, and S. Dasso (2011), Investigating the observational signatures of magnetic cloud substructure, *Journal of Geophysical Research: Space Physics*, *116*(A1), doi:10.1029/2010JA015940, a01106.

Swisdak, M., B. N. Rogers, J. F. Drake, and M. A. Shay (2003), Diamagnetic suppression of component magnetic reconnection at the magnetopause, *Journal of Geophysical Research (Space Physics)*, *108*, 1218, doi:10.1029/2002JA009726.

Swisdak, M., M. Opher, J. F. Drake, and F. Alouani Bibi (2010), The Vector Direction of the Interstellar Magnetic Field Outside the Heliosphere, *Astrophys. J.*, , *710*, 1769–1775, doi:10.1088/0004-637X/710/2/1769.

Author Manuscript

This article is protected by copyright. All rights reserved.

Thomsen, M. F., D. B. Reisenfeld, D. M. Delapp, R. L. Tokar, D. T. Young, F. J. Crary, E. C. Sittler, M. A. McGraw, and J. D. Williams (2010), Survey of ion plasma parameters in Saturn's magnetosphere, *Journal of Geophysical Research (Space Physics)*, *115*, A10220, doi:10.1029/2010JA015267.

Trenchi, L., et al. (2008), Occurrence of reconnection jets at the dayside magnetopause: Double star observations, *Journal of Geophysical Research: Space Physics*, *113*(A7), doi:10.1029/2007JA012774, a07S10.

Varsani, A., C. J. Owen, A. N. Fazakerley, C. Forsyth, A. P. Walsh, M. André, I. Dandouras, and C. M. Carr (2014), Cluster observations of the substructure of a flux transfer event: analysis of high-time-resolution particle data, *Annales Geophysicae*, *32*(9), 1093–1117, doi:10.5194/angeo-32-1093-2014.

Vignes, D., M. H. Acuña, J. E. P. Connerney, D. H. Crider, H. Rème, and C. Mazelle (2004), Magnetic Flux Ropes in the Martian Atmosphere: Global Characteristics, *Space Science Research*, *111*, 223–231, doi:10.1023/B:SPAC.0000032716.21619.f2.

Walker, R. J., and C. T. Russell (1985), Flux transfer events at the jovian magnetopause, *Journal of Geophysical Research: Space Physics*, *90*(A8), 7397–7404, doi:10.1029/JA090iA08p07397.

Wilson, R. J., R. L. Tokar, M. G. Henderson, T. W. Hill, M. F. Thomsen, and D. H. Pontius (2008), Cassini plasma spectrometer thermal ion measurements in Saturn's inner magnetosphere, *Journal of Geophysical Research (Space Physics)*, *113*, A12218, doi:10.1029/2008JA013486.

Author Manuscript

This article is protected by copyright. All rights reserved.

Xiao, C. J., Z. Y. Pu, Z. W. Ma, S. Y. Fu, Z. Y. Huang, and Q. G. Zong (2004), Inferring of flux rope orientation with the minimum variance analysis technique, *Journal of Geophysical Research: Space Physics*, *109*(A11), doi:10.1029/2004JA010594, a11218.

Young, D. T., J. J. Berthelier, M. Blanc, J. L. Burch, A. J. Coates, R. Goldstein, M. Grande, T. W. Hill, R. E. Johnson, V. Kelha, D. J. McComas, E. C. Sittler, K. R. Svenes, K. Szegö, P. Tanskanen, K. Ahola, D. Anderson, S. Bakshi, R. A. Baragiola, B. L. Barraclough, R. K. Black, S. Bolton, T. Booker, R. Bowman, P. Casey, F. J. Crary, D. Delapp, G. Dirks, N. Eaker, H. Funsten, J. D. Furman, J. T. Gosling, H. Hannula, C. Holmlund, H. Huomo, J. M. Illiano, P. Jensen, M. A. Johnson, D. R. Linder, T. Luntama, S. Maurice, K. P. McCabe, K. Mursula, B. T. Narheim, J. E. Nordholt, A. Preece, J. Rudzki, A. Ruitberg, K. Smith, S. Szalai, M. F. Thomsen, K. Viherkanto, J. Vilppola, T. Vollmer, T. E. Wahl, M. Wüest, T. Ylikorpi, and C. Zinsmeyer (2004), Cassini Plasma Spectrometer Investigation, *Space Science Reviews*, *114*, 1–112, doi: 10.1007/s11214-004-1406-4.

Zhang, H., K. K. Khurana, M. G. Kivelson, V. Angelopoulos, Z. Y. Pu, Q.-G. Zong, J. Liu, and X.-Z. Zhou (2008), Modeling a force-free flux transfer event probed by multiple time history of events and macroscale interactions during substorms (themis) spacecraft, *Journal of Geophysical Research: Space Physics*, *113*(A1), doi:10.1029/2008JA013451, a00C05.

Zhang, H., et al. (2010), Evidence that crater flux transfer events are initial stages of typical flux transfer events, *Journal of Geophysical Research: Space Physics*, *115*(A8), doi:10.1029/2009JA015013, a08229.

Author Manuscript

This article is protected by copyright. All rights reserved.

Zhang, H., et al. (2012), Generation and properties of in vivo flux transfer events, *Journal of Geophysical Research: Space Physics*, *117*(A5), doi:10.1029/2011JA017166, a05224.

Zhong, J., et al. (2013), Three-dimensional magnetic flux rope structure formed by multiple sequential x-line reconnection at the magnetopause, *Journal of Geophysical Research: Space Physics*, *118*(5), 1904–1911, doi:10.1002/jgra.50281.

Zieger, B., and K. C. Hansen (2008), Statistical validation of a solar wind propagation model from 1 to 10 AU, *Journal of Geophysical Research (Space Physics)*, *113*, A08107, doi:10.1029/2008JA013046.

Author Manuscript

This article is protected by copyright. All rights reserved.

Figure 1. Illustrations of: a) a cross section of a flux rope showing the TCR region (shaded red), and b) a three-dimensional representation of the layers of a flux rope, where the outer flux is perpendicular to the core axial field. The core axial field is pointed in the right-to-left direction here, which is the intermediate variance direction from MVA, whilst the tangential direction is in the minimum-maximum plane. Panels c-f) show the MAG data for the TCRs ('T'; red-shading) and the FTE ('F'; blue-shading).

Figure 2. The trajectory of the Cassini spacecraft between January 29th and February 10th 2007. The blue arrow shows the start of the interval and the direction of the trajectory. The red arrow marks the FTE location. The large dots represent the start of the day in UT. The smaller dots mark three hour intervals. Left: the X-Z plane (as 'viewed' from dusk) in the Kronocentric-Solar-Magnetospheric (KSM) coordinate system (Sun to the right), with the *Khurana et al.* [2006] magnetospheric field-line model (grey). The top and bottom right panels show the trajectory in the X-Y ('looking down onto the equatorial plane', with the equatorial plane inclined towards the observer on the dayside) and Y-Z (view from the Sun) KSM planes, respectively. The dotted lines show a model magnetopause location using a solar wind dynamic pressure of 0.12 nPa [*Kanani et al.*, 2010].

Author Manuscript

This article is protected by copyright. All rights reserved.

Figure 3. Observations from February 2nd 2007. Vertical black lines separate the different regions. The centers of the TCRs ('T') and FTE-type flux rope ('F') are marked by the red and blue lines respectively. Top-to-bottom are in situ observations: panels a-b) high-energy electrons and protons, respectively (LEMMS); c) omnidirectional low-energy electron flux (ELS), with background and photoelectron flux removed; d) the calculated electron number density (ELS); e) ions from IMS; f-i) the three components (in KRTP) and magnitude of the magnetic field (MAG). "SW" stands for the solar wind, and "M'sheath" for the magnetosheath. The 'Open' region is shaded in grey. "DEF" and "DNF" stand for differential energy and number flux, respectively.

Figure 4. MVA results for the FTE observed at 23:33:55−23:34:21 UT. MVA hodograms are shown in (a-b). The 's' and 'e' represent the 'start' and 'end' of the data. Panels (c-e), show the magnetic field measurements in MVA coordinates, and the eigenvalue and eigenvector values in KRTP coordinates ($\boldsymbol{R}$, $\boldsymbol{\theta}$, $\boldsymbol{\phi}$). Panels (c-e) show the flux rope model (blue), for comparison with the observations (black).

Author Manuscript

This article is protected by copyright. All rights reserved.

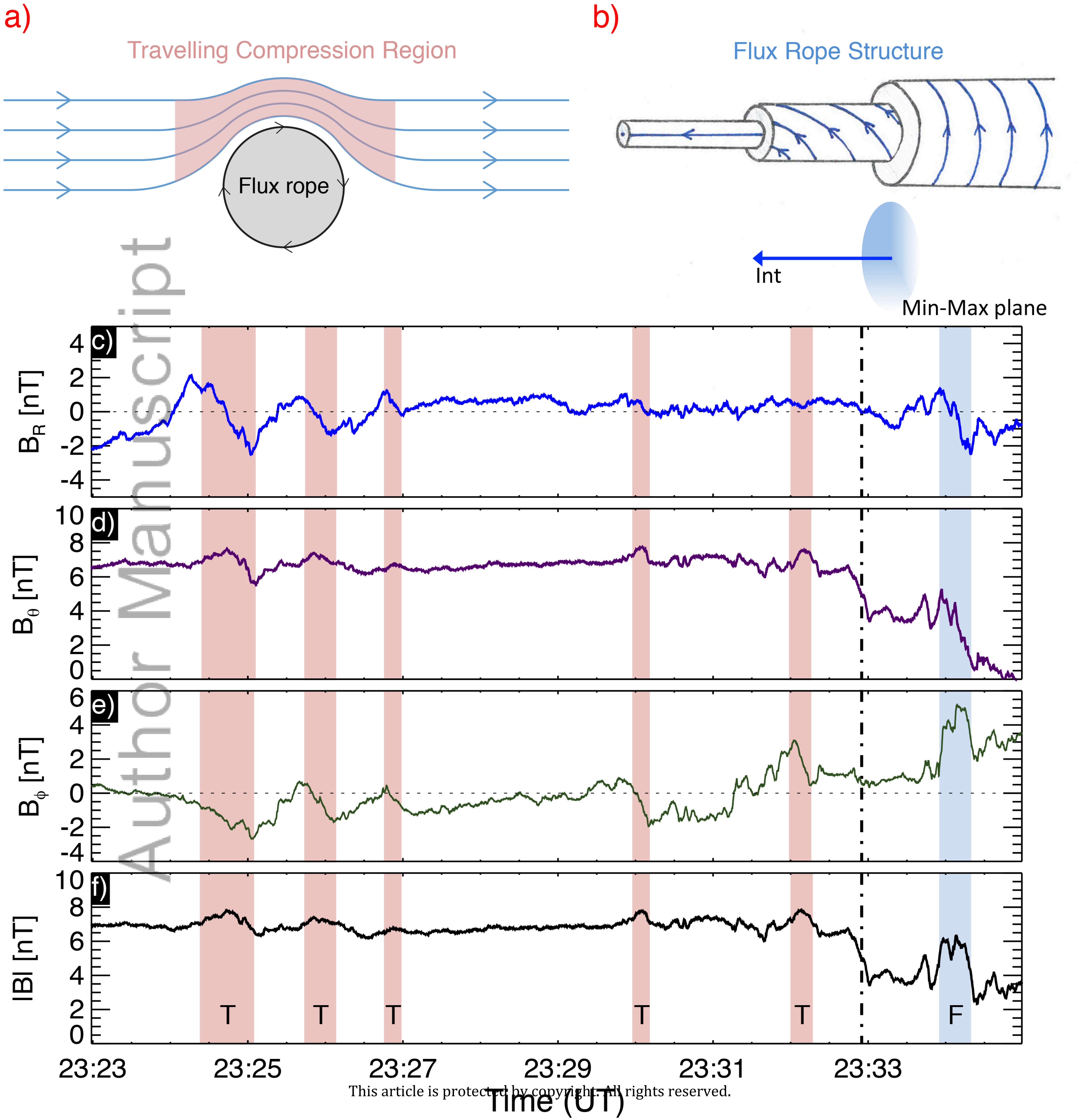

Author Manuscript

This article is protected by copyright. All rights reserved.

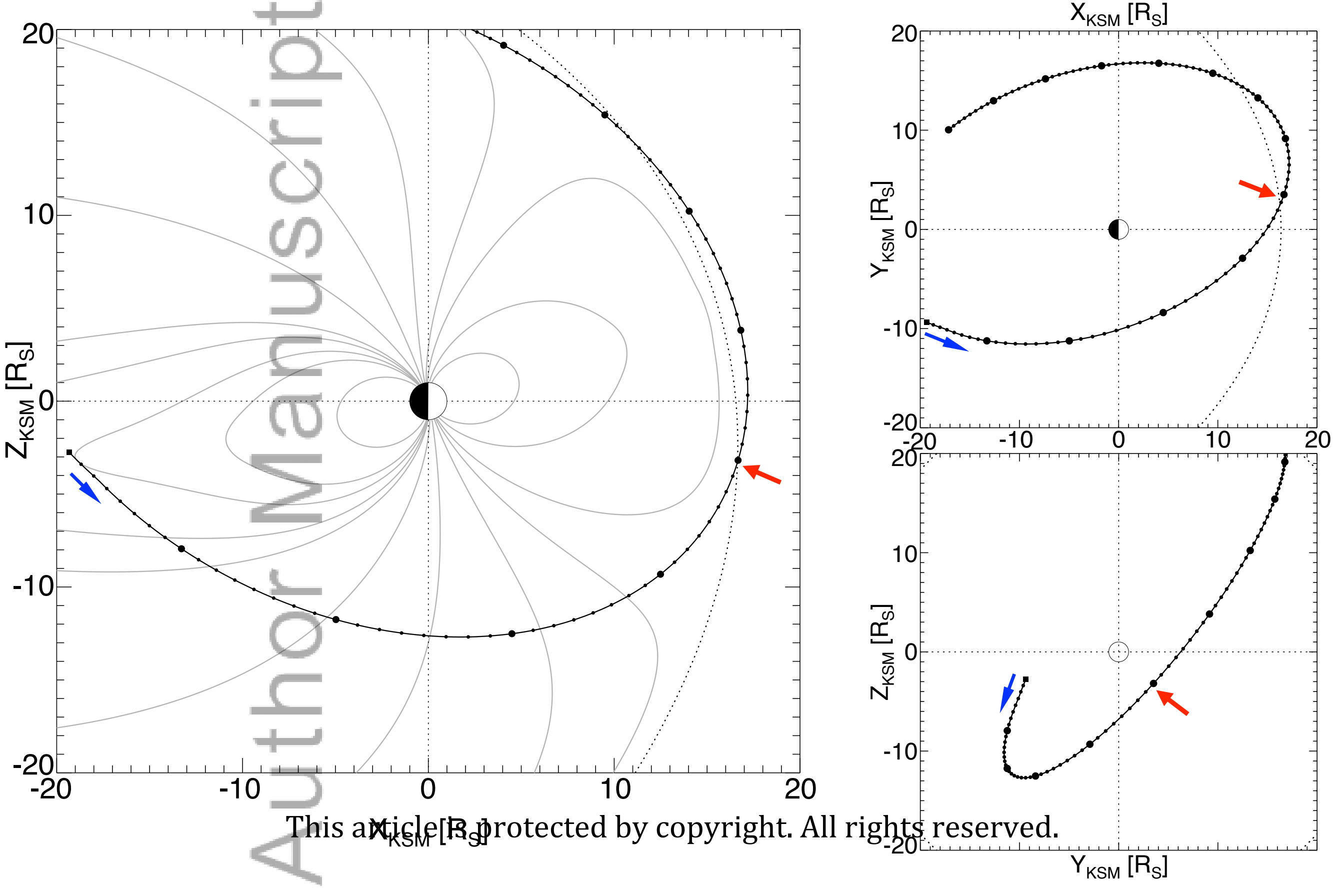

Author Manuscript

This article is protected by copyright. All rights reserved.

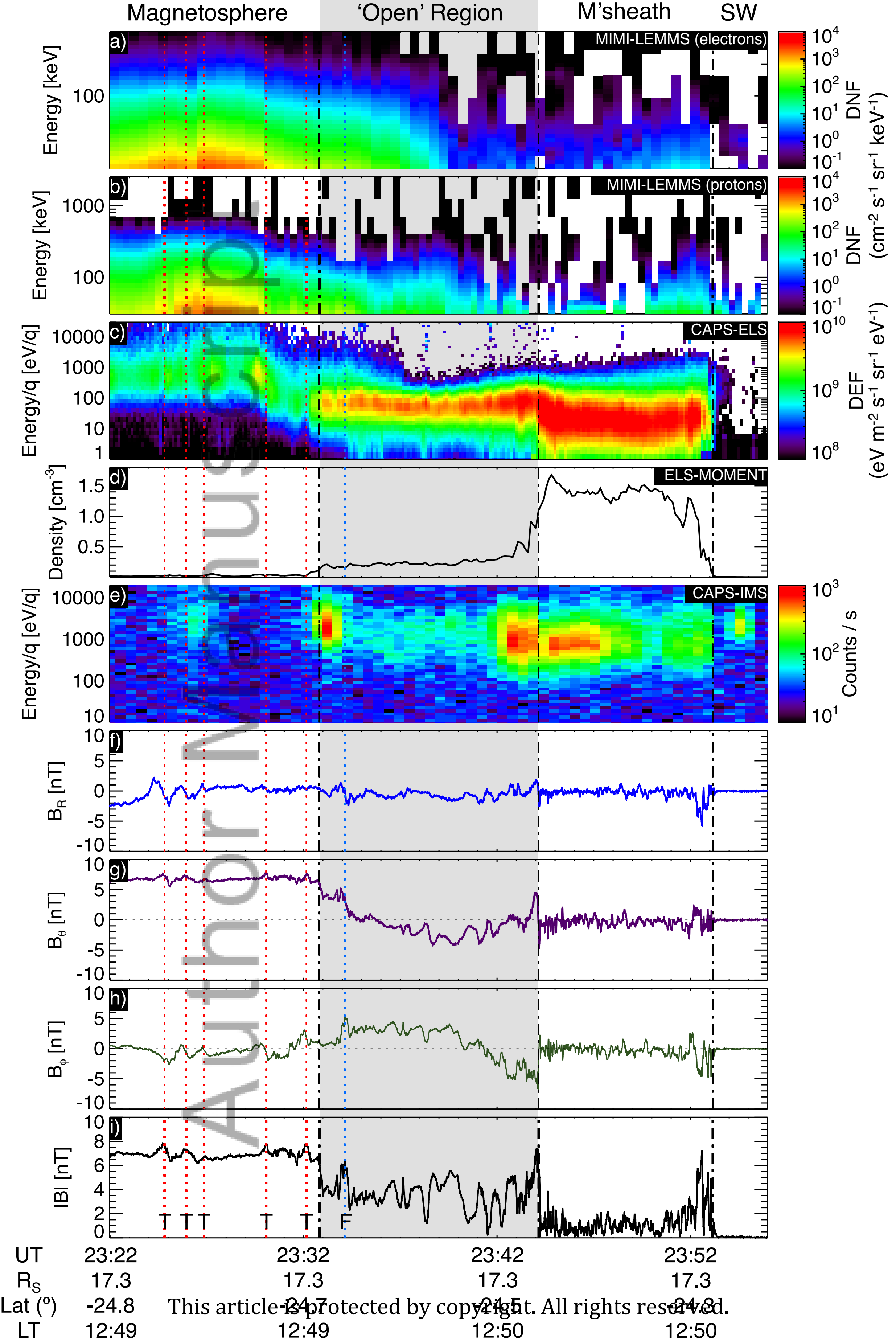

Author Manuscript

This article is protected by copyright. All rights reserved.

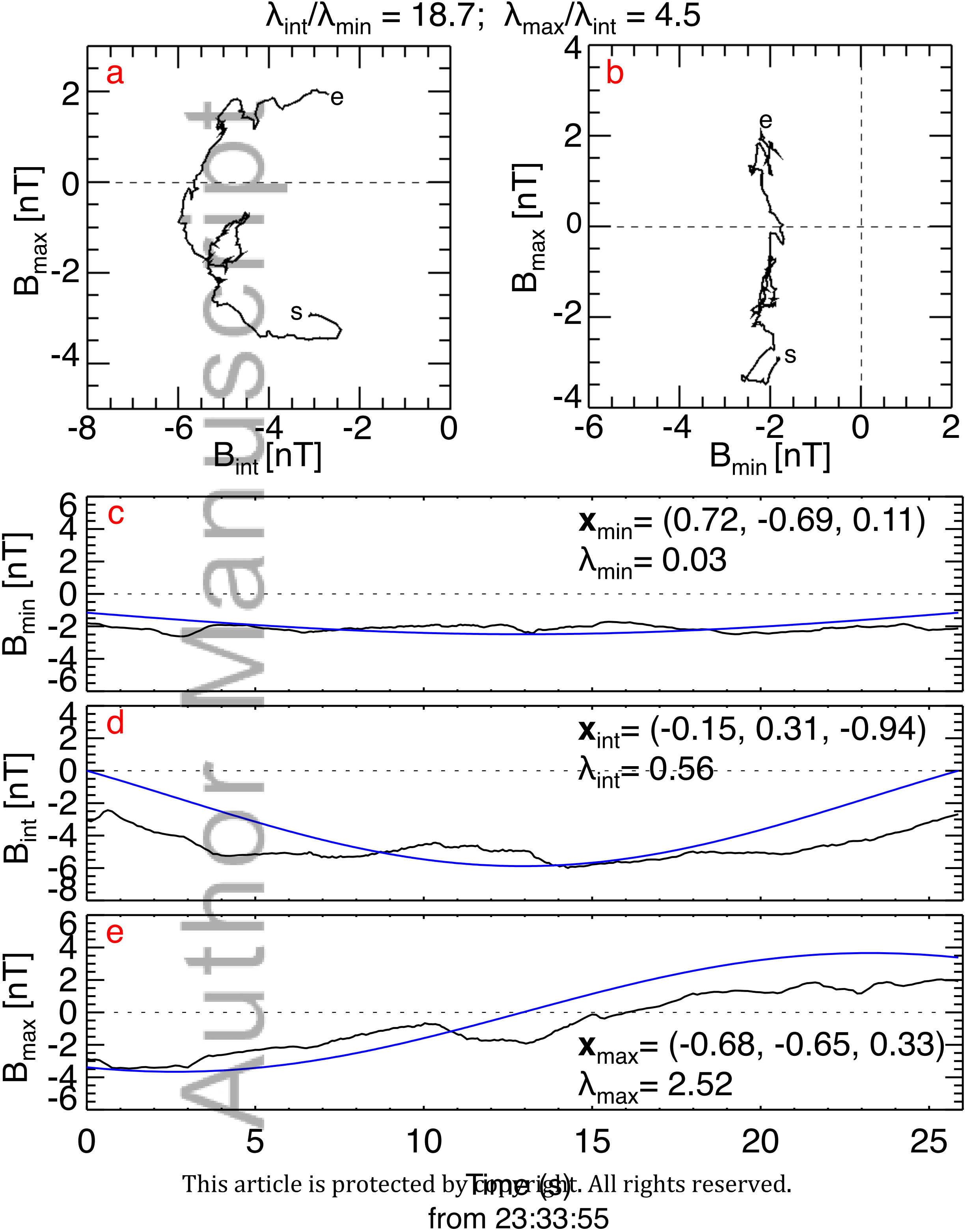

Author Manuscript

This article is protected by copyright. All rights reserved.